

# **Draft Proposal for Vortex-Induced Vibration of Offshore Structures**

**Virginia Polytechnic Institute and State University**  
Blacksburg, VA 24060, USA

May 31, 2003

## Project Objectives

1. Develop a practical and reliable engineering method for the prediction of Vortex-Induced Vibrations (VIV) on offshore slender structures.
2. Develop technical breakthrough in the basic understanding and calculation of VIV and Fluid-Structure Interaction (FSI) for offshore slender structures, such as vertical risers, flexible risers, steel catenary risers, tendons, mooring lines, and pipelines.
3. Develop software modules (and source code) to calculate and simulate VIV on marine slender structures, including hydrodynamic coefficients and fatigue damage.
4. Calibrate theoretical calculations with (a) existing data from participants, (b) new laboratory measurements, and (c) offshore measurement programs.
5. Stimulate worldwide academic and industry research in the VIV area.
6. Train a new cadre of undergraduate and graduate students in the VIV area for possible research and employment.

## Deliverables

1. Software modules, database, and source code to calculate and simulate VIV on marine slender structures, including hydrodynamic coefficients and fatigue damage. For each task, as appropriate, a software module, VPIVIV, including source code and documentation, will be delivered to calculate the lift and drag forces calculated by the proposed method. Since VPIVIV is not a standalone module, participants may use the code with existing finite-element analysis software or special-purpose riser analysis software. The VPIVIV module will be written in C/C++ but a participant may write a wrapper around this module to facilitate their own use and integration of the module; that is, Fortran, DLL (dynamic link library), LIB (library), GUI interface, etc.
2. Technical papers and documents.
3. Short courses, seminars, and discussion of the project results.
4. Consulting expertise.
5. Hold international conferences on VIV.

## Philosophy

1. Focus recent breakthroughs in Computational Fluid Dynamics (CFD), nonlinear dynamics and control, generation of design models using identification techniques, and structural dynamics to understand and quantify the VIV problem.
2. Execute the project in phases that are dependent on participants' technical input and funding levels.
3. Encourage VIV experts to participate and to share knowledge in an effort to stimulate worldwide research.

## Schedule for Phase 1

1. Send out initial description of project to interested companies.
2. Workshop presentation and discussion of project at Virginia Tech.
3. Finalize project plan.
4. Establish founding board.
5. Initiate project including milestones and funding level for each task.

## Organization

1. The project will be directed by the Virginia Tech Nonlinear Vibrations and Fluid Mechanics Laboratories.
2. An advisory/steering committee representing participating organizations.

3. The project liaison is Starmark Offshore Inc. (SOI).
4. Other experts and specialists.
5. Joint-Industry Project (JIP) participants.
6. Other funding sources: NSF, Navy, NASA, etc.

## Approach

Develop technical breakthrough methodologies in the basic understanding and calculation of Vortex-Induced Vibration (VIV) and Fluid-Structure Interaction (FSI) for offshore slender structures, such as vertical risers, flexible risers, steel catenary risers, tendons, mooring lines, and pipelines, by combining numerical simulations using three-dimensional unsteady CFD codes, full-scale and model-scale experimental data, nonlinear dynamics, polyspectral methods, and nonlinear control. Use the detailed fluid-structure-control simulations to generate a database that will be used to develop and calibrate finite-degree-of-freedom (reduced-order) models for design and analysis of VIV problems. Results from this effort will be released to participating organizations during the course of each task. The project will be executed in phases that are dependent on participants' technical input and funding levels.

## Background

Vortex-induced vibrations of offshore marine drilling, production, and export riser systems used in offshore oil and gas operations involve complicated interactions between the riser modes of vibrations and the fluid forces, which might cause structural or fatigue damage under certain situations. As a result of the riser being subjected to currents at high Reynolds numbers, a vortex shedding is produced, resulting in the oscillations of the hydrodynamic loads, which in turn force the riser to vibrate at its natural frequencies. The vortex-shedding frequency may lock on to one of the closest structural natural frequencies. The range over which lock-in or synchronization occurs depends on the oscillation amplitude of the riser. The lock-in can increase the vortex strength, the lift force amplitude, and the mean drag. The amplitude of the riser oscillations can be of the order of its diameter and therefore presents a potent source of fatigue damage. A proper design of the riser system based on a realistic prediction of vortex-induced vibration will reduce risk and may be very cost-effective.

In general, the responses of long risers in highly sheared currents involve nonlinear interactions among the various riser transverse and inline modes (multi-mode or multi-frequency responses) and the complex flowfield. Because the riser transverse and inline motions affect the fluid forces and because these forces, in turn, affect the riser motions, nonlinear interactions between the flow and the riser motions must be considered. An ultimate solution for this problem would be a time-domain numerical simulation of the fluid flow and the riser motion, including the transverse and inline modes of vibration. In this solution, the fluid and the riser would be treated as a single dynamical system and all governing equations would be solved simultaneously and interactively in the time domain. Obviously, this would be impractical because offshore risers may be 3500 *m* or more in length and subjected to sheared currents at high Reynolds numbers. Therefore, for practical reasons, one cannot rely on computational fluid dynamic or experimental techniques for the prediction of the fluid-structure interaction in offshore marine risers and similar slender structures, rather one needs to rely on reduced-order models that take into consideration all of the physical aspects, are validated by a combination of numerical simulation and experiments, and are capable of reliably predicting and simulating vortex-induced vibrations.

Numerous experimental and numerical studies have been carried out on this fluid-structure interaction problem. In spite of these studies, the investigation of this phenomenon is far from complete due largely to the significant nonlinear mechanisms controlling the fluid and the structure. A considerable number of analytical and numerical models have been proposed to evaluate the flow response to the structure vibrations, including wake-oscillator models (Bishop and Hassan, 1964; Hartlen and Currie, 1970; Skop and Griffin, 1973; Iwan and Blevins, 1974; Blevins, 1990). These models consider only the motion of the structure in the transverse direction. By contrast, only few models have been proposed for the inline motion of the structure. Lately, Kim and Perkins (2002) proposed a model that considers coupling of the structure motion in both the transverse and inline directions. In their model, two van der Pol oscillators are employed to account for the

coupling between the lift and drag generated by vortex shedding. The coupling terms are based on the fact that the frequency of the drag oscillations is twice the frequency of the lift. Therefore, they suggested a quadratic coupling between the drag and lift.

The objective of this project is to develop a theoretically and experimentally validated model for single and multiple interacting risers by successive tasks that build upon models for the time variations of the fluid forces, riser transverse and inline modes of vibration, and their interactions. Because experiments are very expensive, we propose to couple our 3-D unsteady Reynolds averaged Navier-Stokes solver to a discretized form of the equations governing the transverse and inline motions of the riser to establish a database. We will then use this database to generate a reduced-order model. Our CFD code is capable of predicting single- and multi-phase flows for Reynolds numbers as high as 10,000,000. This code has been validated using experimental data for Reynolds numbers up to 100,000 (Owis and Nayfeh, 2001, 2002, 2003a, b). The resulting reduced-order model will be validated against available experimental and field data.

## Flow Modeling

In our code, the artificial compressibility method is used to couple the continuity and momentum equations. For turbulence closure, the two-equation model is used. Because of its sensitivity to free-stream conditions, the code switches from the model near the wall to the model away from the wall. The equations are solved on a structured grid using a second-order finite-difference scheme. The convective terms are discretized using a second-order upwind-difference scheme. The physical-time terms, which represent flow unsteadiness, are switched to the right-hand side and used as source terms. These terms are discretized using a second-order three-point backward-difference formula. Different boundary conditions are used in the simulations, including inflow, outflow, and no-slip. All of the boundary conditions are treated implicitly in the code to reduce the restriction on the time step and to increase its stability. At the inflow boundary, the velocity components are specified, while the pressure is extrapolated from the interior points. At the outflow boundary, the pressure

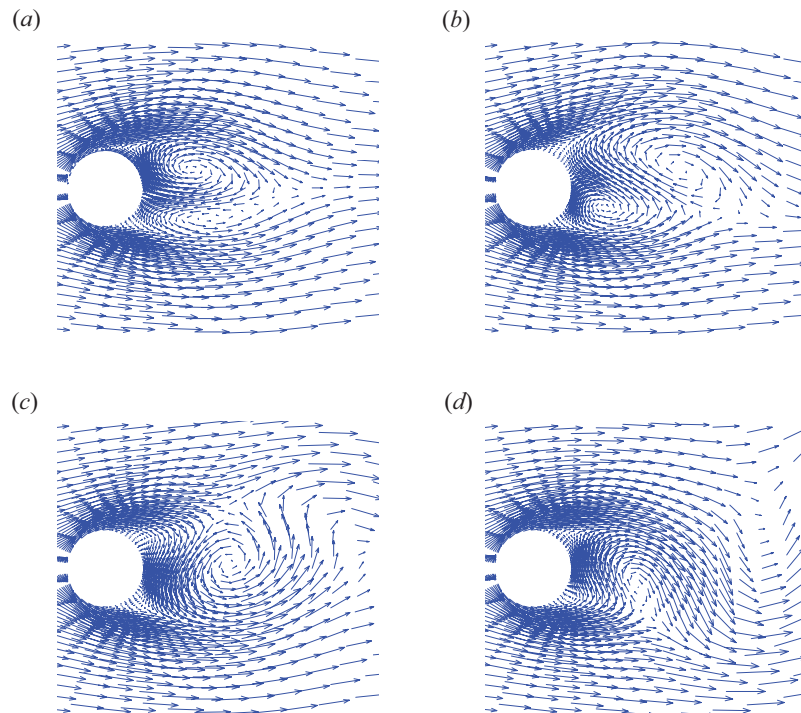


Figure 1: Time snapshots of the velocity vectors in the flowfield over a stationary cylinder at  $Re = 100,000$ .

is specified, whereas the velocity components are extrapolated from the computational domain. On the body surface, the velocities are set equal to its velocity. In addition, similar boundary conditions are set for the turbulence quantities.

An example of the time variations in the flowfield around a circular cylinder is shown in Figure 1. The results clearly show how the vorticity is generated at the separation points over the cylinder with vortices forming in the wake of the cylinder (Figure 1-a). As shown in Figure 1-b, the vorticity generated at the bottom side of the cylinder moves up and cuts the upper vorticity to yield vortex shedding of the upper vortex. This phenomenon is reversed and repeated as shown in Figures 1-c and 1-d, respectively. This reverse in the vorticity yields time variations in the surface pressures over the cylinder (Figure 2) and is the cause for the periodic variations in the lift and drag coefficients. Figure 2 clearly shows the vortex shedding with vortices forming in the near wake and diffusing further downstream.

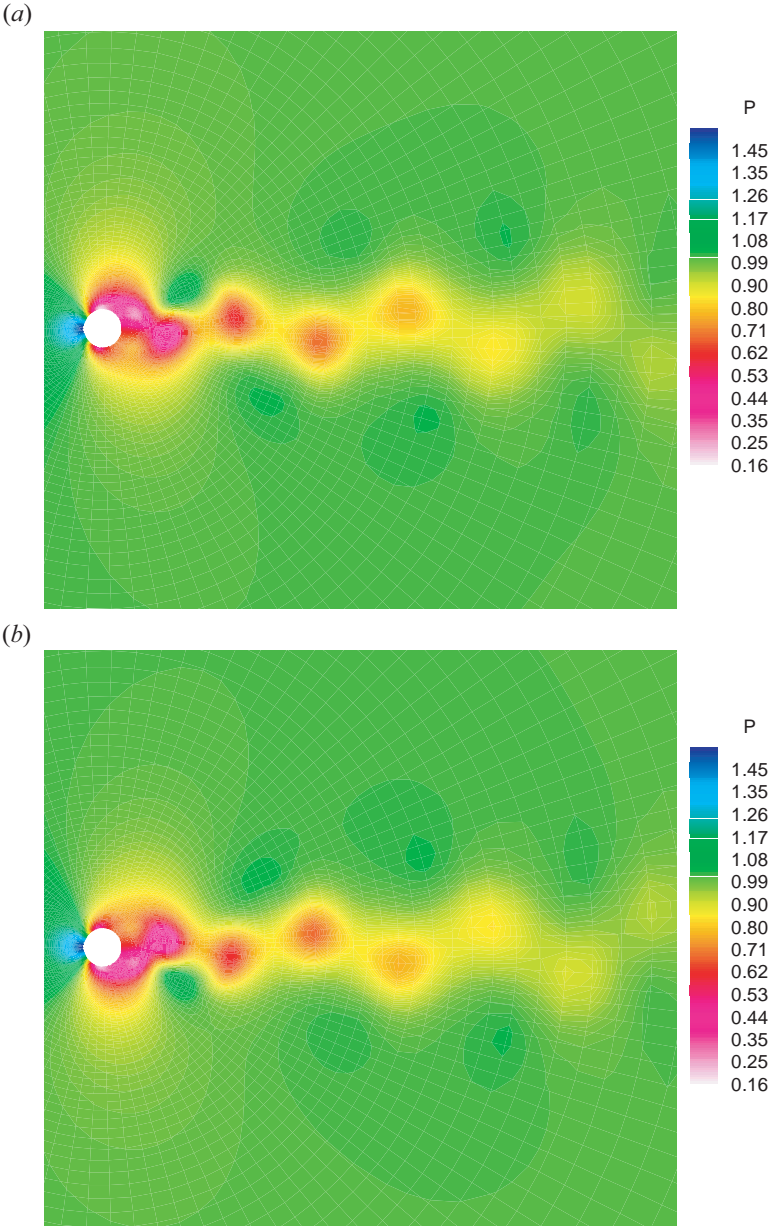


Figure 2: Time snapshots of the pressure contours in the flowfield over a stationary cylinder at  $Re = 100,000$ .

## Modeling of Unsteady Lift and Drag

As a first step to building a reduced-order model, we modeled the time-varying coupled lift and drag forces, which act on a stationary circular cylinder over a wide range of Reynolds numbers. A well-known model for the lift force acting on a circular cylinder when subjected to a fluid flow is the lift wake-oscillator proposed by Hartlen and Currie (1970) who represent the lift by the Rayleigh equation. Currie and Turnball (1987) proposed a similar model for the fluctuations of the drag coefficient. To study resonant responses of suspended elastic cables, Kim and Perkins (2002) modeled the lift by a van der Pol equation with frequency  $\omega_s$  and the drag by another van der Pol equation with frequency  $2\omega_s$  and coupled the two equations nonlinearly. In Kim and Perkins' model, the drag is affected by many possibilities of quadratic couplings with the lift. Additionally, the lift is affected by its quadratic coupling with the drag. These couplings were introduced based on the fact that the main frequency of the drag component is twice the main frequency of the lift component.

Using a combination of perturbation analysis, higher-order spectral moments, and time series of the lift coefficient obtained from the CFD code, we developed a model of the lift and drag and identified the coefficients in the model equations. We describe below the methodology.

First, we integrated the pressure at the cylinder surface to determine the lift and drag coefficients. In Figures 3 and 4, we show the spectra of the lift and drag coefficients at two representative Reynolds numbers, namely 20,000 and 100,000, respectively. At  $Re = 20,000$ , the spectrum of the lift coefficient shows a major peak at the shedding frequency  $f = 0.237$ . At  $Re = 100,000$ , the peak is at  $f = 0.254$ .

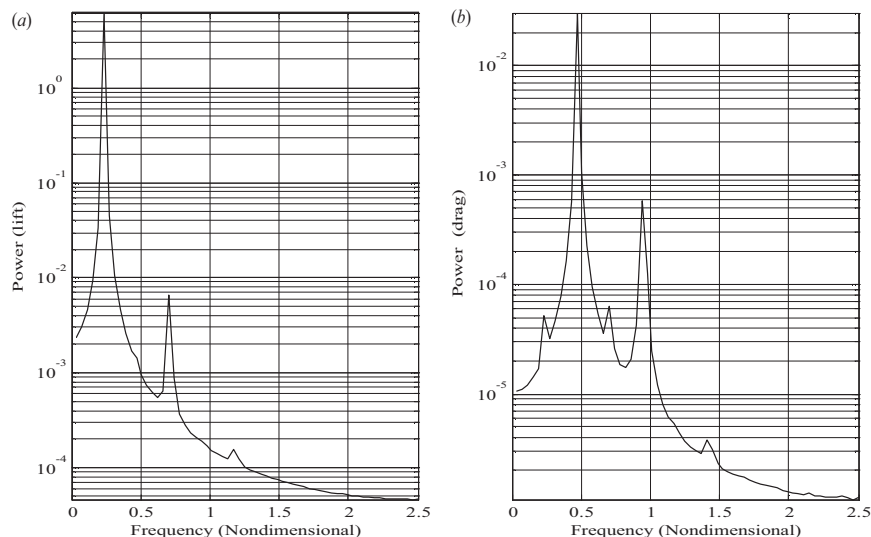


Figure 3: Lift and drag spectra for a flowfield over a stationary cylinder at  $Re = 20,000$ .

In addition to the major peak at  $f$ , there is a peak in the lift spectrum at  $3f$  in each of Figures 3 and 4. It is three to four orders of magnitude smaller than the major peak at  $f$ . The presence of peaks corresponding to the shedding frequency and its third harmonic suggests that the lift coefficient  $l$  on the circular cylinder can be modeled by either the Rayleigh equation or the van der Pol equation. The Rayleigh equation is

$$\ddot{l} + \omega_s^2 l = \mu_r \dot{l} - \alpha_r l^3 \quad (1)$$

The van der Pol equation is

$$\ddot{l} + \omega_s^2 l = \mu_v \dot{l} - \alpha_v l^2 \dot{l} \quad (2)$$

In these equations,  $\omega_s$  is the shedding frequency of the stationary cylinder,  $\mu$  and  $\alpha$  represent the linear and nonlinear damping coefficients, and the subscripts  $r$  and  $v$  are used to denote these coefficients in the Rayleigh and van der Pol equations, respectively. Also,  $\mu$  and  $\alpha$  are positive so that the linear damping is

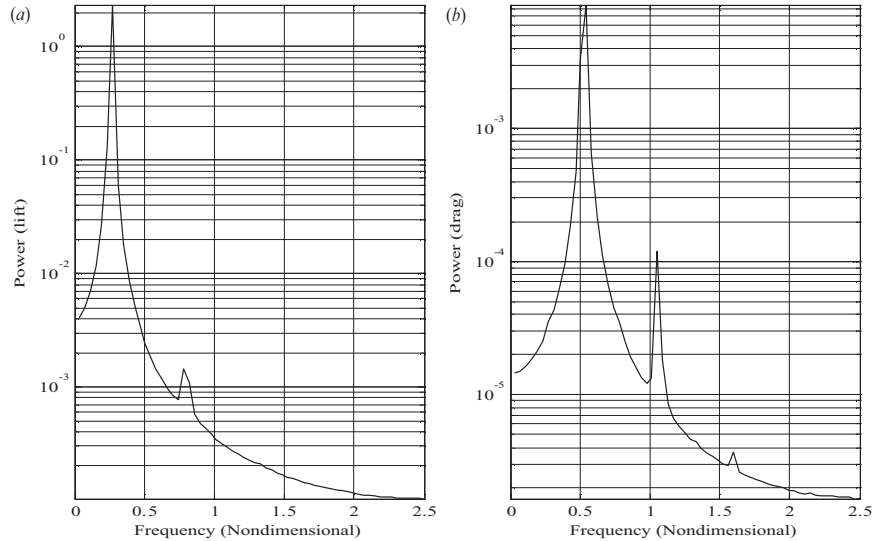


Figure 4: Lift and drag spectra for a flowfield over a stationary cylinder at  $Re = 100,000$ .

negative and the nonlinear damping is positive. As a result, small motions grow and large motions decay, resulting in stable limit cycles. It is of interest to note also that the van der Pol equation can be obtained by differentiating the Rayleigh equation once with respect to time and performing a derivative substitution.

Using the method of multiple scales (Nayfeh, 1973, 1981), we obtain the following approximate solution of Eq. (1):

$$l \approx a \cos(\omega_s t + \beta) + \frac{\alpha_r \omega_s}{32} a^3 \cos\left(3\omega_s t + 3\beta - \frac{1}{2}\pi\right) \quad (3)$$

where  $\beta$  is a constant phase and

$$\dot{a} = \frac{1}{2}\mu_r a - \frac{3\alpha_r \omega_s^2}{8} a^3 \quad (4)$$

Using separation of variables, we find that the solution of Eq. (4) is given by

$$a^2 = \frac{4\mu_r}{3\alpha_r \omega_s^2 + e^{-\mu_r(t+c)}} \quad (5)$$

As  $t \rightarrow \infty$ , it follows from Eq. (5) that

$$a \rightarrow \frac{2}{\omega_s} \sqrt{\frac{\mu_r}{3\alpha_r}} \quad (6)$$

Similarly, using the method of multiple scales, we obtain the following approximate solution of Eq. (2):

$$l \approx a \cos(\omega_s t + \beta) + \frac{\alpha_v}{32\omega_s} a^3 \cos\left(3\omega_s t + 3\beta + \frac{1}{2}\pi\right) \quad (7)$$

where  $\beta$  is a constant phase and

$$\dot{a} = \frac{1}{2}\mu_v a - \frac{\alpha_v}{8} a^3 \quad (8)$$

Using separation of variables, we find that the solution of Eq. (8) is given by

$$a^2 = \frac{4\mu_v}{\alpha_v + e^{-\mu_v(t+c)}} \quad (9)$$

As  $t \rightarrow \infty$ , it follows from Eq. (9) that

$$a \longrightarrow 2\sqrt{\frac{\mu_v}{\alpha_v}} \quad (10)$$

As presented above, Eqs. (3) and (7) show a difference in the phase of the third harmonic in relation to the phase of the component at the vortex shedding frequency. Determining this phase will yield the correct modeling equation for the lift coefficient. In order to do so, and based on the lift spectra of Figures 3 and 4, we represent the lift as

$$l \approx a_1 \cos(\omega_s t) + a_3 \cos(3\omega_s t + \gamma) \quad (11)$$

where  $\omega_s$  is the shedding frequency,  $a_1$  is the amplitude of the component at  $\omega_s$ ,  $a_3$  is the amplitude at  $3\omega_s$ , and  $\gamma$  represents the phase of the third harmonic when the phase  $\beta$  of the fundamental component is zero. Comparing Eq. (11) with Eqs. (3) and (7), we conclude that the lift can be modeled by either the Rayleigh or the van der Pol equation, depending on whether  $\gamma \approx -\frac{1}{2}\pi$  or  $\gamma \approx \frac{1}{2}\pi$ . Consequently, to match the time series predicted with the van der Pol or Rayleigh equation with that obtained from the numerical simulation, one needs to determine accurately the amplitudes  $a_1$  and  $a_3$  as well as the phase  $\gamma$ . Because the phase  $\gamma$  is defined as the phase of the third harmonic when the phase of the vortex shedding frequency is zero, it can be recovered, at any time, by the phase relation (Hajj et al., 1993)  $\gamma = \phi(3\omega_s) - 3\phi(\omega_s)$  where  $\phi(\omega_s)$  and  $\phi(3\omega_s)$  are, respectively, the phases of the components at the vortex shedding frequency and its third harmonic. This relation can be measured as the phase of the auto-trispectrum between these two components, which is defined as

$$S_{lll} = \langle L(3f)L^*(f)L^*(f)L^*(f) \rangle \quad (12)$$

where  $L(f)$  is the Fourier Transform of the lift time series  $l(t)$ ,  $L^*(f)$  is the complex conjugate, and  $\langle \dots \rangle$  denotes ensemble averaging. Thus, the Fourier transform of the time series derived from the numerical simulation yields the amplitudes of the peaks at the vortex shedding frequency and its third harmonic and their phase relation.

We carried out many CFD calculations for few Reynolds numbers, calculated the pressure and drag, and then calculated their power spectra and auto-trispectrum. In Table 1, we show variations of the shedding frequency  $f$ ,  $a_1$ , and  $a_3$  with the Reynolds number. We note that the nondimensional vortex shedding frequency  $f$ , or Strouhal number, is in agreement with experimental results for the Reynolds number 200. For the higher Reynolds numbers, the Strouhal number is overestimated. This is most likely due to the increased three-dimensional effects (Mittal and Balachandar, 1995). We note that the results for the Reynolds number 1,000,000 are not unique because the flow is transitional.

Table 1: Lift parameters as a function of the Reynolds Number.

Re	$f$	$a_1$	$a_3$
200	0.193	0.6184	0.0044
1,000	0.2295	1.205	0.039
2,000	0.2368	1.394	0.052
10,000	0.2391	1.793	0.049
20,000	0.2368	1.728	0.055
40,000	0.2510	1.465	0.040
100,000	0.2538	1.056	0.021
500,000	0.2656	1.121	0.025
1,000,000	0.2550	1.321	0.033

As for the drag coefficient  $d$ , the spectra in Figures 3 and 4 show that, in each case, the drag has two peaks at the second and fourth harmonics of the vortex shedding frequency; that is,

$$d(t) = d_m + a_2 \cos(2\omega_s t + \gamma_2) + a_4 \cos(4\omega_s t + \gamma_4) \quad (13)$$

where  $d_m$  is the mean drag. Because the drag and lift are the result of the pressure distribution on the surface of the cylinder, it is feasible to relate the drag to the lift directly. The fact that the major component in the spectrum of the drag coefficient is at twice the shedding frequency suggests that the drag is a quadratic function of the lift; that is, the drag is proportional to either  $l^2$ ,  $\dot{l}^2$ , or  $l\dot{l}$ . Of these three forms, the correct form must yield the right phase relation between the drag and the lift. Because the frequency of the major component of the drag is twice the frequency of the major component in the lift, this phase relation is given by  $\phi(2\omega_s)$  in the drag time series  $-2\phi(\omega_s)$  in the lift time series. As shown by Hajj et al. (1993), this phase can be measured as the phase of the cross bispectrum between  $2f$  in the drag and  $f$  in the lift, which is defined as

$$S_{dl} = \langle D(2f)L^*(f)L^*(f) \rangle \quad (14)$$

where  $D(2f)$  is the Fourier Transform of the drag time series  $d(t)$ .

The time series for the lift and drag coefficients obtained from the numerical solutions were analyzed to determine the parameters discussed above. We note that the sampling frequency and record length had to be adjusted between the different runs in order to accurately predict the amplitudes of the main frequencies and the phase relations between them. For the lift time series, the phase of  $S_{lll}$  is approximately  $\frac{1}{2}\pi$  for all runs and hence the van der Pol equation is the appropriate model for the lift. By comparing Eq. (11) with Eqs. (7) and (10), we find that

$$\alpha_v = \frac{32\omega_s a_3}{a_1^3} \quad (15)$$

$$\mu_v = \frac{1}{4}\alpha_v a_1^2 \quad (16)$$

These equations are then used to determine the linear and nonlinear damping coefficients in the van der Pol equation from the amplitude of the Fourier components in the time series.

The drag consists of two components. The first is a mean component that is independent of the lift and the second is a periodic component that is related to the unsteady lift. Because the phase relation  $\gamma_2$  between the drag component and the lift as defined above is near  $\frac{3}{2}\pi$  in all records, the periodic component of the drag must be proportional to  $-l\dot{l}$ . Consequently, the drag coefficient can be modeled by

$$d = d_m - \frac{a_2}{\omega_s a_1^2} l\dot{l} \quad (17)$$

Variation with the Reynolds number of the mean drag  $d_m$ , obtained independently as a mean value from the time series of the drag, and of the coefficient  $k_1$ , which is the amplitude of the major frequency component in the drag, is shown in Table 2. We note that the spectrum of  $d$  calculated from Eq. (17) yields the same drag spectrum calculated from the CFD code, such as those shown in Figures 3 and 4.

Table 2: Drag parameters as a function of the Reynolds number.

Re	$d_m$	$a_2$	$a_4$
200	1.18	0.0368	0.00066
1,000	1.29	0.135	0.0105
2,000	1.36	0.175	0.0231
10,000	1.62	0.129	0.0201
20,000	1.48	0.112	0.0168
40,000	1.32	0.0786	0.0101
100,000	0.85	0.0636	0.0072
500,000	0.80	0.0709	0.0077
1,000,000	1.06	0.0773	0.0098

The parameters in Tables 1 and 2 were used to estimate  $\mu_v$  and  $\alpha_v$ . These values were then used in conjunction with Eqs. (2) and (17) to predict the steady-state lift and drag. A comparison of the simulated

and modeled lift and drag coefficients at  $Re = 200, 20,000$  and  $100,000$  is shown in Figures 5-7. Obviously, the results show excellent agreement at all Reynolds numbers.

As we showed above, the time-varying coupled lift and drag coefficients acting on a circular cylinder can be modeled. Numerical solutions of the unsteady Reynolds-Averaged Navier-Stokes equations were obtained to generate a database for the model. Spectral analysis of the time series of the lift coefficient showed that it contains a major component at the vortex shedding frequency and a smaller one at its third harmonic, implying the use of either the Rayleigh or the van der Pol equation to model the lift. Approximate solutions of both equations showed that only one of these equations can be used to model the lift. This is dependent on the phase relation between the two frequency components. Measurement of this phase relation with the auto-trispectrum showed that the lift can be modeled only by the van der Pol equation. Frequency domain analysis of the drag showed that it contains the second and fourth harmonics of the vortex shedding frequency, implying that the drag is a quadratic function of the lift. Using the phase of the cross-bispectrum between the drag and lift time series, it was determined that the unsteady component of the drag must be proportional to  $l^2$  where  $l$  is the lift coefficient. The models and results presented here are a first step in the development of a reduced-order model for vortex-induced vibrations that includes the cylinder's motions.

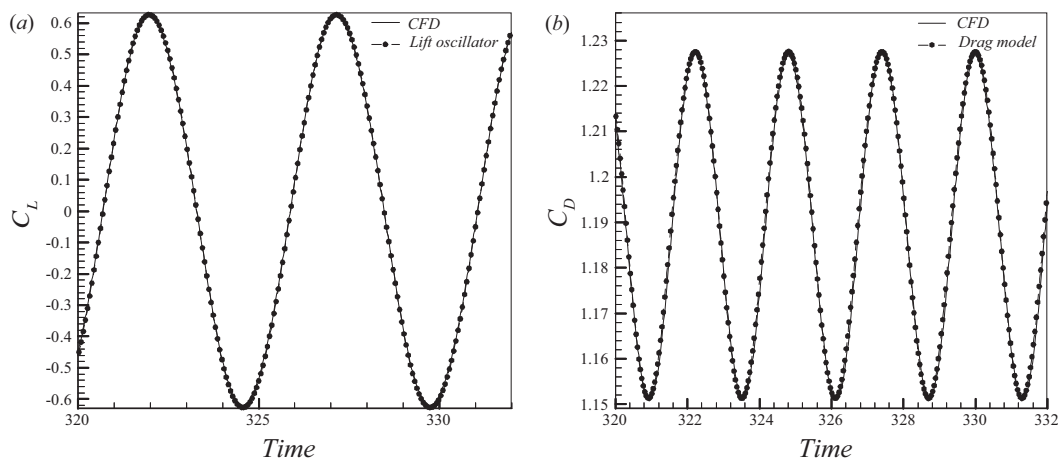


Figure 5: Comparisons between the simulated and modeled lift and drag coefficients ( $Re=200$ ).

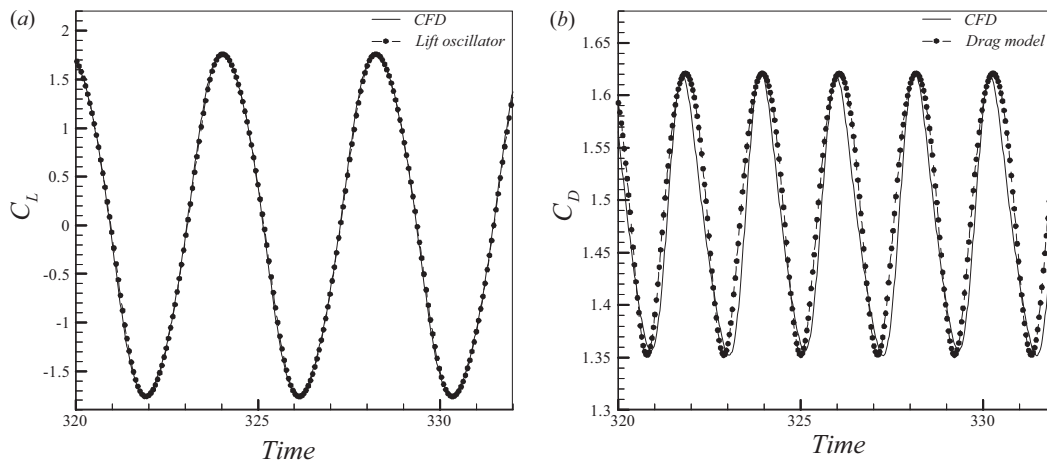


Figure 6: Comparisons between the simulated and modeled lift and drag coefficients ( $Re=20,000$ ).

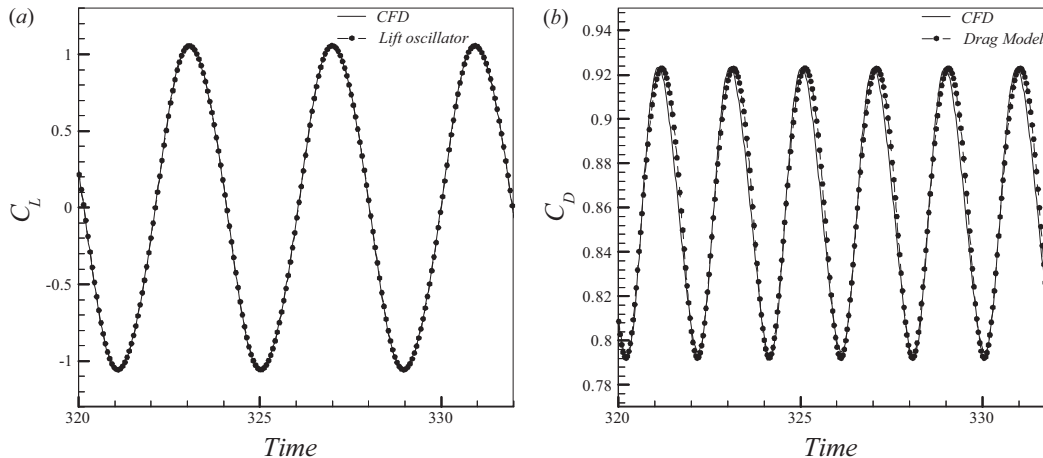


Figure 7: Comparisons between the simulated and modeled lift and drag coefficients ( $Re=100,000$ ).

## References

- Bishop, R. E. D. and Hassan, A. Y., 1964, "The lift and drag forces on a circular cylinder oscillating on a flowing fluid," *Proceedings of the Royal Society of London, Series A* **277**, 51-75.
- Blevins, R. D., 1990, *Flow-Induced Vibration*, Van Nostrand Reinhold, New York.
- Crespo da Silva, M. R. M., 1988, "Non-linear flexural-flexural-torsional-extensional dynamics of beams – II. Response analysis," *International Journal of Solids and Structures* **24**, 1235-1242.
- Currie, I. G. and Turnbull, D. H., 1987, "Streamwise oscillations of cylinders near the critical Reynolds number," *Journal of Fluids and Structures* **1**, 185-196.
- Hajj, M. R., Miksad, R. W., and Powers, E. J., 1993, "Fundamental-subharmonic interaction: Effect of phase relations," *Journal of Fluid Mechanics* **256**, 403-426.
- Hartlen, R. T. and Currie, I. G., 1970, "Lift-oscillator model of vortex-induced vibration," *ASCE Journal of the Engineering Mechanics* **96**, 577-591.
- Iwan, W. D. and Blevins, R. D., 1974, "A model for vortex-induced oscillation of structures," *Journal of Applied Mechanics* **41**, 581-586.
- Kim, W. J. and Perkins, N. C., 2002, "Two-dimensional vortex-induced vibration of cable suspensions," *Journal of Fluids and Structures* **16**(2), 229-245.
- Mittal, R. and Balachandar, S., 1995, "Effect of three-dimensionality on the lift and drag of nominally two-dimensional cylinders," *Physics of Fluids* **7**(8), 1841-1865.
- Nayfeh, A. H., 1973, *Perturbation Methods*, Wiley, New York.
- Nayfeh, A. H., 1981, *Introduction to Perturbation Techniques*, Wiley, New York.
- Owis, F. M. and Nayfeh, A. H., 2001, "Numerical simulation of super- and partially-cavitating flows over a axisymmetric projectile," in *Proceedings of the 39th AIAA Aerospace Sciences Meeting and Exhibit*, **AIAA Paper No. 2001-1042**, Reno, NV, January 8-11.
- Owis, F. M. and Nayfeh, A. H., 2002, "A compressible multi-phase flow solver for the computation of the supercavitation over high-speed torpedo," in *Proceedings of the 40th AIAA Aerospace Sciences Meeting and Exhibit*, **AIAA Paper No. 2002-0875**, Reno, NV, January 13-17.
- Owis, F. M. and Nayfeh, A. H., 2003a, "Computations of the compressible multi-phase flow over the cavitating high speed torpedo," *Journal of Fluids Engineering* (accepted for publication).
- Owis, F. M. and Nayfeh, A. H., 2003b, "Numerical simulation of 3-d incompressible, multi-phase flows over cavitating projectiles," *European Journal of Mechanics - B/Fluids* (submitted for publication).
- Skop, R. A. and Griffin, O. M., 1973, "A model for the vortex-excited resonant response of bluff cylinders," *Journal of Sound and Vibration* **27**, 225-233.



## Technical Plan

To accomplish the overall project objectives, we anticipate the following tasks over a period of two years:

### Year I

#### Task 1. An Infinite Stationary Cylinder in a Uniform Flow

We will create a comprehensive data base for Reynolds numbers as high as 10,000,000 to calculate the transient as well as the steady-state lift and drag coefficients by integrating the van der Pol equation using parameters from the data base. To this end, we will

1. Run the CFD code for a fixed cylinder for many Reynolds numbers.
2. Compute the shedding frequency  $\omega_s$  and the amplitudes of the lift components  $a_1$  and  $a_3$  using the FFT.
3. Compute the drag amplitudes  $a_2$  and  $a_4$  and the mean drag  $d_m$ .
4. Build an extensive database for the coefficients  $\omega_s$ ,  $\alpha_v$ ,  $\mu_v$ ,  $d_m$ , and  $a_2$  for many Reynolds numbers. This database can be used to calculate variation of the transient and steady-state lift and drag coefficients with Reynolds number.

#### Task 2. An Infinite Cylinder Oscillating Transversely to a Uniform Flow

We will quantify the influence of the cylinder motions, both transverse (cross current) and inline, on the lift and drag coefficients. We denote the inline and transverse directions by  $x$  and  $y$ , respectively. We start with specified transverse harmonic motions of the form

$$\dot{y} = A \cos(\Omega t) \quad (18)$$

where  $\dot{y}$  is the cylinder velocity,  $A$  is the amplitude of oscillation, and  $\Omega$  is the frequency of oscillation. In this case, we expect the van der Pol Eq. (2) to be modified to

$$\ddot{l} + \omega_s^2 l = \mu_v \dot{l} - \alpha_v l^2 \dot{l} + F(y, \dot{y}, \ddot{y}) \quad (19)$$

where the function  $F$  is determined by running the CFD code and analyzing the data as follows:

1. We select a Reynolds number,  $A$ , and  $\Omega$ .
2. We run the CFD code, calculate the flowfield, including the pressure.
3. We integrate the pressure to determine the lift and drag coefficients.
4. We calculate the spectra of the lift and drag coefficients.
5. We inspect the spectra to determine whether  $F$  is a linear or nonlinear function.
6. We calculate the different orders of spectral moments between  $y$  and  $l$  to determine the function  $F$ .
7. We solve Eq. (19) with various values of the coefficients, compare the result with the CFD results, and identify the coefficients.
8. We compare the spectrum of the drag coefficient with that of the lift coefficient to ascertain how to modify the drag model given by Eq. (17).
9. We repeat the process for many values of  $A$  and  $\Omega$  to establish a data base.
10. We repeat steps 1-9 for many Reynolds numbers to establish a comprehensive base from which one can calculate the lift and drag coefficients for a cylinder oscillating transversely in a uniform current.

#### Task 3. An Infinite Cylinder Oscillating Inline to a Uniform Flow

We start with specified inline harmonic motions of the form

$$\dot{x} = A \cos(\Omega t) \quad (20)$$

where  $\dot{x}$  is the cylinder velocity,  $A$  is the amplitude of oscillation, and  $\Omega$  is the frequency of oscillation. In this case, we expect the van der Pol equation, Eq. (2), to be modified to

$$\ddot{l} + \omega_s^2 l = \mu_v \dot{l} - \alpha_v l^2 \dot{l} + G(x, \dot{x}, \ddot{x}) \quad (21)$$

where the function  $G$  is determined by running the CFD code and analyzing the data as follows:

1. We select a Reynolds number,  $A$ , and  $\Omega$ .
2. We run the CFD code, calculate the flowfield, including the pressure.
3. We integrate the pressure to determine the lift and drag coefficients.
4. We calculate the spectra of the lift and drag coefficients.
5. We inspect the spectra to determine whether  $G$  is a linear or nonlinear function.
6. We calculate the different orders of spectral moments between  $x$  and  $l$  to determine  $G$ .
7. We solve Eq. (21) with various values of the coefficients, compare the result with the CFD results, and identify the coefficients.
8. We compare the spectrum of the drag coefficient with that of the lift coefficient to ascertain how to modify the drag model given by Eq. (17).
9. We repeat the process for many values of  $A$  and  $\Omega$  to establish a database.
10. We repeat steps 1-9 for many Reynolds numbers to establish a comprehensive base from which one can calculate the lift and drag coefficients for a cylinder oscillating transversely in a uniform current.

#### Task 4. Interaction of Transverse Motion of a Cylinder with a Uniform Flow

In Tasks 2 and 3, the cylinder motion is specified. In this task, we will quantify the interaction of transverse motions of a cylinder with a uniform flow. The cylinder is restrained in the inline direction and free to oscillate in response to the flow in the transverse (cross current) direction. As aforementioned, we denote the transverse direction by  $y$ . The equation describing the motion of the cylinder can be expressed

$$\ddot{y} + \omega_y^2 y = \frac{1}{2} \rho U^2 \Gamma l + F_y(y, \dot{y}, \ddot{y}) \quad (22)$$

where  $\omega_y$  is the natural frequency of oscillation of the cylinder,  $\Gamma$  is a constant, and  $F_y$  represents the radiation damping, nonlinear stiffness, and added mass. The lift coefficient continues to be described by

$$\ddot{l} + \omega_s^2 l = \mu_v \dot{l} - \alpha_v l^2 \dot{l} + F(y, \dot{y}, \ddot{y}) \quad (23)$$

We will generate a code to solve simultaneously and interactively in the time domain for the transverse motion of the cylinder and the surrounding flow. Because the hydrodynamic load depends on the velocity and acceleration of the cylinder, we will use a predictor-corrector method rather than a Runge-Kutta method. Then, we will use the code to determine  $F_y$  as follows:

1. We select a Reynolds number and  $\omega_y$ .
2. We run the simulation to calculate the flowfield, including the pressure on the cylinder and the transverse motion of the cylinder.
3. We integrate the pressure to determine the lift and drag coefficients.
4. We calculate the spectra of the lift and drag coefficients and the cylinder motion.
5. We inspect the spectra to determine whether  $F_y$  is a linear or a nonlinear function.
6. We calculate the different orders of spectral moments between  $y$  and  $l$  to determine  $F_y$ .
7. We solve Eqs. (22) and (23) with various values of the coefficients, compare the result with the simulation results, and identify the coefficients.
8. We repeat the process for many values of  $\omega_y$  and Reynolds number to establish a database.

#### Task 5. Interaction of Inline Motion of a Cylinder with a Uniform Flow

In this task, we will quantify the interaction of inline motions of a cylinder with a uniform flow. The cylinder is restrained in the transverse direction and free to oscillate in response to the flow in the inline direction. As aforementioned, we denote the inline direction by  $x$ . The equation describing the motion of the cylinder can be expressed

$$\ddot{x} + \omega_x^2 x = \frac{1}{2} \rho U^2 \Gamma d + F_x(x, \dot{x}, \ddot{x}) \quad (24)$$

where  $\omega_x$  is the natural frequency of oscillation of the cylinder,  $\Gamma$  is a constant, and  $F_x$  represents the radiation damping, nonlinear stiffness, and added mass. The lift coefficient continues to be described by

$$\ddot{l} + \omega_s^2 l = \mu_v \dot{l} - \alpha_v l^2 \dot{l} + G(x, \dot{x}, \ddot{x}) \quad (25)$$

where the drag is related to the lift by Eq. (17).

We will generate a code to solve simultaneously and interactively in the time domain for the inline motion of the cylinder and the surrounding flow. Because the hydrodynamic load depends on the velocity and acceleration of the cylinder, we will use a predictor-corrector method rather than a Runge-Kutta method. Then, we will use the code to determine  $F_x$  as follows:

1. We select a Reynolds number and  $\omega_x$ .
2. We run the simulation to calculate the flowfield, including the pressure on the cylinder and the transverse motion of the cylinder.
3. We integrate the pressure to determine the lift and drag coefficients.
4. We calculate the spectra of the lift and drag coefficients and the cylinder motion.
5. We inspect the spectra to determine whether  $F_x$  is a linear or a nonlinear function.
6. We calculate the different orders of spectral moments between  $x$  and  $l$  to determine  $F_x$ .
7. We solve Eqs. (22) and (23) with various values of the coefficients, compare the result with the simulation results, and identify the coefficients.
8. We repeat the process for many values of  $\omega_x$  and Reynolds number to establish a database.

### Task 6. Interaction of Transverse and Inline Motions of a Cylinder with a Uniform Flow

In Tasks 4 and 5, the cylinder was restrained to move in one direction only (either the transverse or inline). In this task, we will quantify the interaction of transverse and inline motions of a cylinder with a uniform flow. The equations describing the motion of the cylinder can be expressed

$$\ddot{y} + \omega_y^2 y = \frac{1}{2} \rho U^2 \Gamma l + F_y(y, \dot{y}, \ddot{y}) + G_y(y, \dot{y}, \ddot{y}, x, \dot{x}, \ddot{x}) \quad (26)$$

$$\ddot{x} + \omega_x^2 x = \frac{1}{2} \rho U^2 \Gamma d + F_x(x, \dot{x}, \ddot{x}) + G_x(y, \dot{y}, \ddot{y}, x, \dot{x}, \ddot{x}) \quad (27)$$

where  $\omega_y$  and  $\omega_x$  are the natural frequencies of oscillation of the cylinder in the transverse and inline directions, and  $\Gamma$  is a constant, and  $F_y$  represents the radiation damping, nonlinear stiffness, and added mass. The lift coefficient continues to be described by

$$\ddot{l} + \omega_s^2 l = \mu_v \dot{l} - \alpha_v l^2 \dot{l} + F(y, \dot{y}, \ddot{y}) + G(x, \dot{x}, \ddot{x}) + H(y, \dot{y}, \ddot{y}, x, \dot{x}, \ddot{x}) \quad (28)$$

We will generate a code to solve simultaneously and interactively in the time domain for the transverse and inline motions of the cylinder and the surrounding flow by using a predictor-corrector method. Then, we will use the code to determine  $G_x$ ,  $G_y$ , and  $H$  as in the preceding tasks.

### Task 7. Finite-Element Method Analysis Coupled with Local van der Pol Models

We will represent the incoming continuous sheared flow with a flow composed of many segments of uniform flows. We will determine the Reynolds number over each segment and hence the parameters for the lift and the drag. Then, we use a finite-element code to discretize the riser and couple the resulting ordinary-differential equations governing the dependent variables at each node with the van der Pol equation and the drag model. The resulting system of equations will be integrated in the time domain to determine simultaneously the riser deflections and the distribution of the hydrodynamic loads. The output of this task will be a module that can be coupled with existing finite-element riser codes.

The module will numerically integrate the van der Pol equation (or similar model) using the database of generated coefficients at a specified riser arc length point  $s$ . Typical input to the module include for point  $s$ : (1) specified point  $s$ ; (2) riser properties; (3) current state of the riser (i.e., displacements, velocities, acceleration, etc.); (4) flow field conditions; and (5) specified integration time  $t$ . The output from the module will include the calculated lift and drag forces or coefficients. In the event that the user employs a nonlinear solver or predictor-corrector routine, the user must manage, maintain, store, and recall the state of the module inputs.

## Task 8. Reduced-Order Model with Local van der Pol Models

Instead of coupling the lift and drag models with the dependent variable at the nodes, we will use the finite-element code to calculate the mode shapes and frequencies of the riser. Then, we will use the Galerkin procedure and express the riser inline  $v(z, t)$  and transverse  $w(z, t)$  deflections as

$$v(z, t) = \sum_{m=1}^M \phi_m(z) x_m(t) \quad \text{and} \quad w(z, t) = \sum_{m=1}^M \psi_m(z) y_m(t) \quad (29)$$

where  $\phi_m(z)$  and  $\psi_m(z)$  are the  $m$ th structural mode shapes in the inline and transverse directions, respectively. Moreover, we will project the local hydrodynamic loads in each segment on the mode shapes. Then, we will solve the resulting ordinary-differential equations governing the  $x_m(t)$  and  $y_m(t)$  simultaneously with the van der Pol equations and drag models in the different segments to determine the riser deflections and distribution of the hydrodynamic loads. The output of this task will be a module that can be used by existing finite-element representations of riser systems.

The module will numerically integrate the van der Pol equation (or similar model) using the database of generated coefficients at a specified riser arc length point  $s$ . Typical input to the module include for point  $s$ : (1) specified point  $s$ ; (2) riser properties; (3) current state of the riser (i.e., displacements, velocities, acceleration, etc.); (4) flow field conditions; and (5) specified integration time  $t$ . The output from the module will include the calculated lift and drag forces or coefficients. In the event that the user employs a nonlinear solver or predictor-corrector routine, the user must manage, maintain, store, and recall the state of the module inputs.

## Year II

### Task 9. Correlation of Vortices in a Sheared Flow

We will run the three-dimensional version of our CFD code to calculate the three-dimensional flow over a cylinder in a sheared flow to investigate the correlation of the shed vortices. We will attempt to model the lift and drag analytically by extending, and possibly refining, the 2-D flow model of Eqs. (28) and (17) for the lift and drag coefficients, respectively. To this end, we seek to model the lift coefficient  $l(z, t)$  along the cylinder by

$$\frac{\partial^2 l}{\partial t^2} + \omega_s^2 l = \mu_v \frac{\partial l}{\partial t} - \alpha_v l^2 \frac{\partial l}{\partial t} + \lambda \frac{\partial^2 l}{\partial z^2} + F(w, \dot{w}, \ddot{w}) + G(v, \dot{v}, \ddot{v}) + H(w, \dot{w}, \ddot{w}, v, \dot{v}, \ddot{v}) \quad (30)$$

and propose that the drag coefficient  $d(z, t)$  along the cylinder is described by the form

$$d = d_{mean} - Kl \frac{\partial l}{\partial t} \quad (31)$$

We will use the code to determine the dependence of  $\lambda$ ,  $F$ ,  $G$ ,  $H$ , and  $K$  on  $z$ .

### Task 10. Multimodal Interactions in Flexible Risers

In Tasks 2 and 3, the cylinder is treated as a rigid body moving in either direction. In Tasks 4-6, the motion of the cylinder is described using a single mode in each direction and the motion may be uni-directional or bi-directional.

In practice, risers are distributed-parameter systems that are quite slender and very flexible. Moreover, they experience sheared flows, so that the lift and drag coefficients may vary along the span as well as in time. Therefore, the motions of these structures are often comprised of many modes. Moreover, because such slender structures may exhibit large deflections, they are nonlinear in nature. And, due to nonlinear couplings, multi-modal interactions among the different transverse and inline modes might occur, which result in complex and large-amplitude vibrations that could significantly degrade or fatigue the structure. To this end, we propose to investigate the influence of multi-modal interactions in a flexible riser under VIV.

Depending on the boundary conditions, the equations of motion describing the riser can take different forms. Assuming that the bottom end (at  $z = 0$ ) is restricted from longitudinal (axial) movement, the

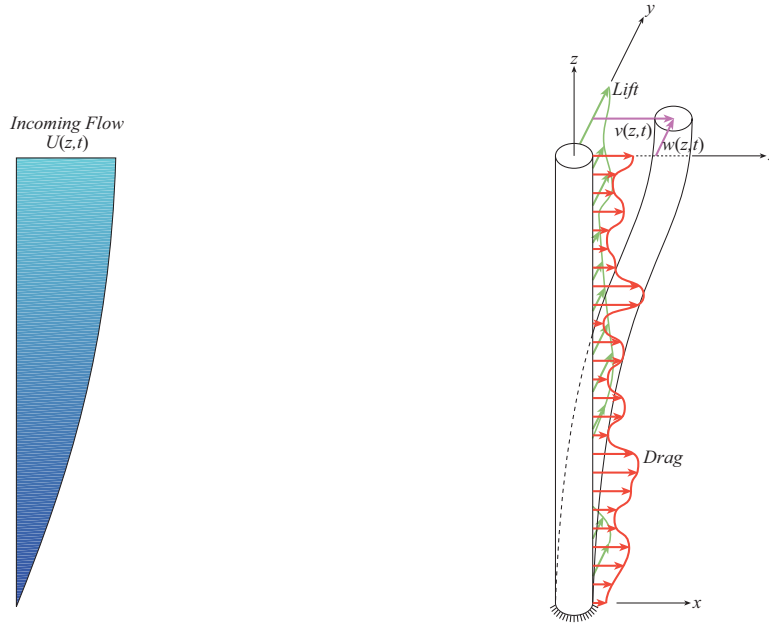


Figure 9: A sketch of a cylinder element under lift and drag forces.

transverse and inline motions of the cylinder can be described by a nonlinear partial-differential system of the form (Crespo da Silva, 1988):

$$m \frac{\partial^2 w}{\partial t^2} - N w'' + (EI w'')'' = Q_w - EI [w' (v' v'' + w' w'')]'' + \left( \frac{K_u}{1 + K_u} \right) \frac{EA}{2L} \left[ w'' \int_0^L (v'^2 + w'^2) dz \right] - \frac{1}{2} m \left\{ w' \int_L^z \frac{\partial^2}{\partial t^2} \left[ \int_0^z (v'^2 + w'^2) dz \right] dz \right\}' \quad (32)$$

$$m \frac{\partial^2 v}{\partial t^2} - N v'' + (EI v'')'' = Q_v - EI [v' (v' v'' + w' w'')]'' + \left( \frac{K_u}{1 + K_u} \right) \frac{EA}{2L} \left[ v'' \int_0^L (v'^2 + w'^2) dz \right] - \frac{1}{2} m \left\{ v' \int_L^z \frac{\partial^2}{\partial t^2} \left[ \int_0^z (v'^2 + w'^2) dz \right] dz \right\}' \quad (33)$$

where  $v(z, t)$  and  $w(z, t)$  are the in-line and transverse deflections, respectively, along the  $x$  and  $y$  coordinates,  $Q_v$  stands for non-conservative in-line forces acting on the riser,  $Q_w$  stands for non-conservative transverse forces acting on the riser,  $N$  is an applied axial tensioning force which might be time varying,  $m$  is the mass per unit length,  $E$  is the modulus of elasticity, and  $L$ ,  $A$ , and  $I$  are, respectively, the length, cross-section area, and moment of inertia of the riser. The forces  $Q_v$  and  $Q_w$  represent the loads generated by the flow, waves, and wind. Equations (32) and (33) are nonlinear, containing cubic geometric and inertia terms due to mid-plane stretching and large deflections, which couple the in-line and transverse motions. The parameter  $K_u$  is a spring coefficient that quantifies the degree of axial restraint at the top end (at  $z = L$ ). These equations are coupled to the Navier-Stokes equations

$$\nabla \cdot \mathbf{v} = 0 \quad (34)$$

$$\frac{\partial \mathbf{v}}{\partial t} + \mathbf{v} \cdot \nabla \mathbf{v} = -\frac{\nabla p}{\rho} + \nabla \cdot (\mu \nabla \mathbf{v}) \quad (35)$$

where  $\mathbf{v}$  is the flow velocity vector,  $p$  is the pressure field,  $\rho$  is the fluid density, and  $\mu$  is the viscosity. Moreover, Eqs. (32) and (33) are augmented by the appropriate boundary conditions, such as clamped or pinned at the ends. The flow boundary conditions demand that the relative velocity of the fluid to the

velocity of the riser be zero (i.e., no slip and no penetration) and the velocity of the fluid approaches the incoming stream far away from the riser.

One approach to solving for the fluid-structure interaction problem is to discretize Eqs. (32) and (33) using a number of modes sufficient to accurately describe the different possible responses. That is, we express the displacements as in Eq. (29). Furthermore, we discretize the lift and drag coefficients by projecting them onto the mode shapes as follows:

$$Q_{Drag}(w, v; z, t) = \sum_{m=1}^M \phi_m(z) D_m(w, v; t) \quad \text{and} \quad Q_{Lift}(w, v; z, t) = \sum_{m=1}^M \psi_m(z) L_m(w, v; t) \quad (36)$$

The result is a set of  $2 \times M$  nonlinear second-order ordinary-differential equations of the form

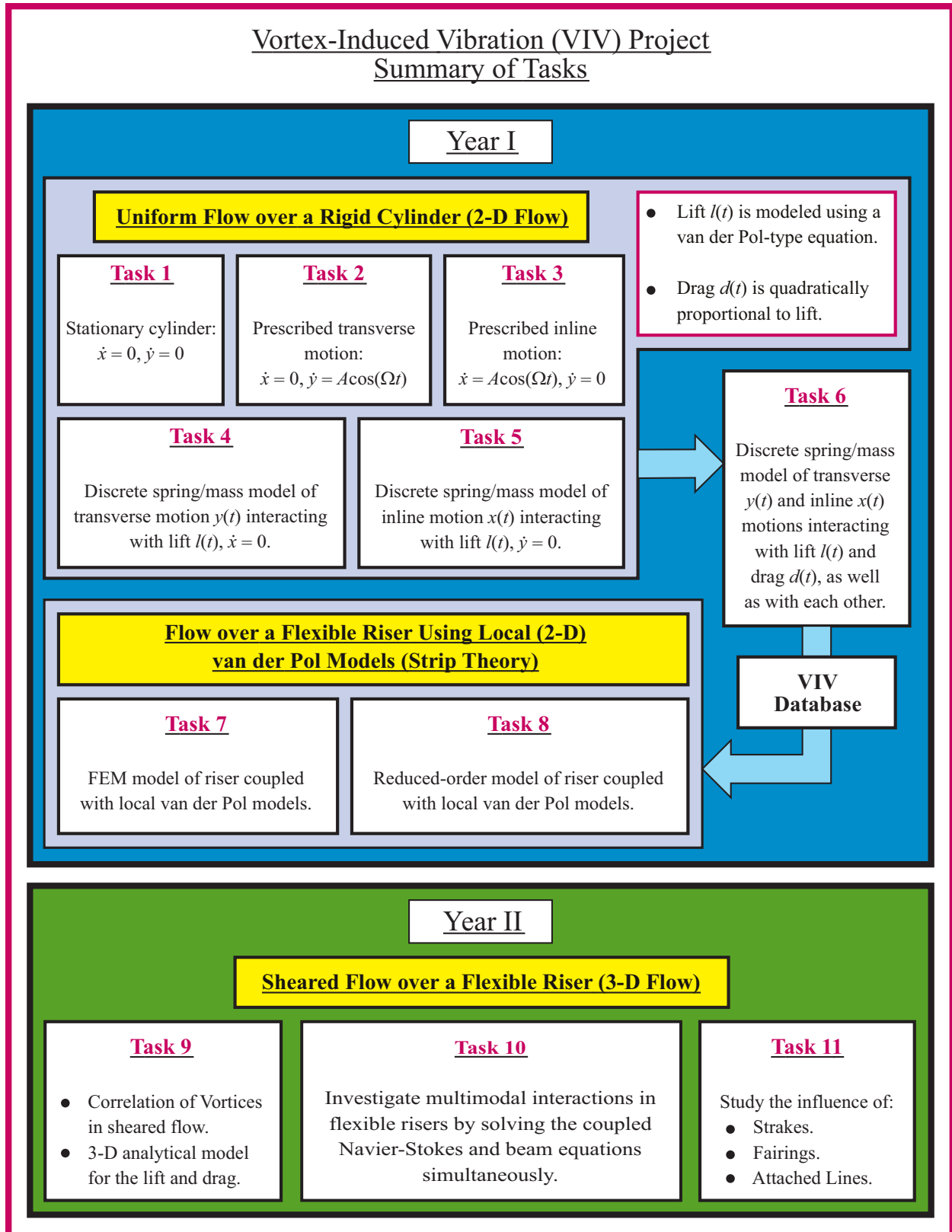
$$\ddot{y}_m + \omega_{ym}^2 y_m = L_m(\mathbf{y}, \dot{\mathbf{y}}, \ddot{\mathbf{y}}, \mathbf{x}, \dot{\mathbf{x}}, \ddot{\mathbf{x}}) + G_{ym}(\mathbf{x}, \mathbf{y}) \quad (37)$$

$$\ddot{x}_m + \omega_{xm}^2 x_m = D_m(\mathbf{y}, \dot{\mathbf{y}}, \ddot{\mathbf{y}}, \mathbf{x}, \dot{\mathbf{x}}, \ddot{\mathbf{x}}) + G_{xm}(\mathbf{x}, \mathbf{y}) \quad (38)$$

where  $\mathbf{x}$  and  $\mathbf{y}$  are  $M$ -dimensional vectors of the generalized coordinates  $x_j$  and  $y_j$ , which must be solved simultaneously with the Navier-Stokes equations. It is well known that the vortex shedding and flow patterns can be significantly influenced by the amplitude and direction of the riser's motion, which, in turn, modify the riser's oscillations, and so on. That is, the flow feeds energy into the structure and vice versa. Therefore, it is necessary to solve the CFD code together with Eqs. (37) and (38) for the transverse and inline motions of the riser and the surrounding flow interactively by using a predictor-corrector numerical integration method. A challenge would be to adaptively map (or mesh) the fluid forces onto the riser at each time step.

### Task 11. Strakes, Fairings, and In-Flow Turbulence

We will use the 3-D CFD code to evaluate the influence of the strakes, fairings, attached lines, and in-flow turbulence.



Year II

**Sheared Flow over a Flexible Riser (3-D Flow)**

Task 9

- Correlation of Vortices in sheared flow.
- 3-D analytical model for the lift and drag.

Task 10

Investigate multimodal interactions in flexible risers by solving the coupled Navier-Stokes and beam equations simultaneously.

Task 11

Study the influence of:

- Strakes.
- Fairings.
- Attached Lines.

Figure 10: Breakdown of the proposed tasks for the Vortex-Induced Vibration Project.